Renewable Energy, Environment, and Power Quality Journal (REE&PQJ)
ISSN:3020-531X
Volume 26, July 2026

Line Protection in Power-Electronic-Dominated Networks Using the α-Plane: Analysis and Performance Evaluation

B. Agudelo-Cruz, M. Alzate-Posso and S. Pérez-Londoño

ICE[3] Research Group, Electrical Engineering Program
Universidad Tecnológica de Pereira
Campus la Julita, 660003, Pereira, Colombia. colxiver.agudelo, marcos.alzate, saperez@utp.edu.co

Abstract

This paper presents an evaluation of α-plane-based line differential protection when applied to power systems with high penetration of inverter-based resources (IBRs). A detailed electromagnetic transient model of the test system was developed in PSCAD/EMTDC. Fault scenarios considering different fault resistances and locations, fault types, and sampling frequencies were evaluated. The measured current signals were used as inputs to assess the performance of the α-plane-based line differential protection, considering both the non-adaptive and adaptive implementations. Based on the results, the analysis identifies fault conditions under which line differential protection schemes exhibit performance limitations in inverter-dominated networks. Particular emphasis is placed on single-phase-to-ground, two-phase-to-ground, and three-phase-to-ground fault scenarios. The results offer valuable insights into the interaction between IBR dynamics and α-plane-based line differential protection, highlighting key challenges related to reduced fault-current levels, transient behaviour, and measurement uncertainties. Based on these findings, this paper provides guidance on the design, implementation, and configuration of modern line differential protection schemes for power systems with high penetration of IBR.

Key words: Inverter-based resources, Power system protection, Fault Analysis, Line differential protection.

1. Introduction

The integration of IBRs affects the performance and reliability of conventional protection schemes. Furthermore, the IBRs fault behaviour, influenced by internal control mechanisms, complicates the detection and coordination of protection systems originally designed for networks dominated by synchronous generators. This may result in protective relays failing to operate correctly during fault conditions or operating inappropriately, thereby compromising the sensitivity and stability of protection systems [1, 2]. Line differential protection also faces challenges in conventional power networks, including synchronisation issues, cybersecurity concerns, capacitive effects, loading conditions, weak-infeed conditions, and power-line-related issues [2].

1.1 State of art

Mainly, grid-following inverters rely on the power network to establish voltage and frequency references through phase-locked loops (PLLs). During disturbances and fault conditions, this characteristic may induce oscillations and grid control interaction phenomena that degrade system stability and alter the electrical quantities measured by protection devices [3, 4]. Consequently, conventional relays may experience coordination failures, unwanted tripping, or insensitivity to internal faults, due to the limited fault current contribution of IBRs and the harmonic distortions associated with converter control [1, 2]. Several adaptive line protection strategies have been developed for overcurrent, distance, and differential schemes. Optimisation-based approaches have been reported to adjust pickup currents and coordination times in order to preserve selectivity under variations of the IBRs fault current contribution for directional overcurrent protection [5]. However, distance protection may be limited in weak infeed scenarios, for example, when a line connects a strong source at one end and a weak or renewable-based source at the other. Under such conditions, the apparent impedance may shift and fall outside the predefined operating zones [6]. Considering the limitations of overcurrent and distance approaches, line differential protection (ANSI 87L) stands out by comparing currents at both terminals, which provides high effectiveness for internal faults and selectivity under external fault conditions. Nevertheless, in systems with IBRs, its reliability may be degraded by disturbances in unfaulted phases and by the low-impedance zero-sequence paths in transformers. These effects impair phase discrimination and compromise the stability of the operating characteristic [7, 8].

Among advances aimed at strengthening the differential criterion, techniques such as the α-plane have been reported. For example, a current mapping strategy is used to redefine differential and restraint currents by transforming these measurements at both line terminals. This complex-domain representation can produce more stable trajectories and improve sensitivity and separation between internal and external faults in the presence of IBRs [9]. Additionally, current transformer saturation remains a critical challenge; fast saturation detection logics and algorithms have been proposed to dynamically adjust sensitivity under external fault conditions, thereby mitigating spurious operations during the initial stages of the event [10].

Recent literature has also explored next-generation approaches, such as setting-less protection, based on dynamic state estimation and statistical testing used to verify in real time the consistency between measurements and physical component models. These strategies aim to reduce dependence on fixed parameter settings and to enhance performance under varying operating conditions, including networks with high converter penetration [11]. Additionally, several adaptive approaches have been proposed for line differential protection, as presented in [12]; these algorithms adjust the protection zones based on the current state of the power system. Finally, algorithm testing under IBR conditions has not been widely reported.

1.2 Contributions

The most important contributions of this paper are: a) Analysis of the performance of non-adaptive and adaptive α-plane based line differential protection in IBR polluted power systems; b) Determination of the influence of the type of fault, sampling frequency, fault location, and fault resistance on the performance of the differential protection.

2. α-plane–based line differential protection

Conventional α-plane–based line differential protection is used due to its robustness. This method is based on the geometric representation of the current ratio measured at both ends of the line (C_R), as expressed in (1) where $\tilde{I}_L$ and $\tilde{I}_R$ denote the phasor currents measured at the local and remote terminals of the line; enabling discrimination between internal and external faults through regions defined in the complex plane, as illustrated in Fig. 1a [13].

$$C_R = \frac{\tilde{I}_R}{\tilde{I}_L} = |C_R|\, e^{j\alpha} \tag{1}$$

Under normal operating conditions or during external faults, the value of C_R is located near $(-1,0)$ in an α plane, reflecting currents of similar magnitude and opposite phase. In the presence of an internal fault, the relationship between the currents is significantly altered, causing the ratio trajectory to leave the restraint region and move towards the operating region. This behaviour enables the correct operation of the relay [13, 14].

In the α-plane, the restraint region is defined by two boundaries: an outer (R) and an inner radius ($1/R$) that delimit the admissible range of the current ratio magnitude. The steady-state operating condition is characterised by equation (2).

$$\frac{1}{R} \leq |C_R| \leq R \tag{2}$$

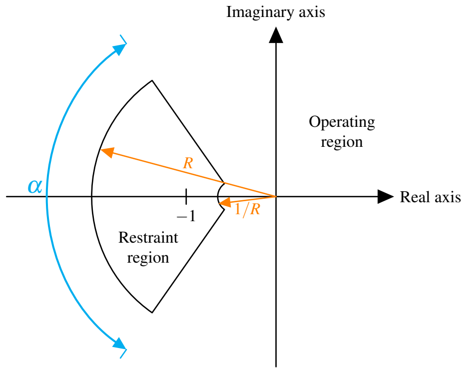

(a) α-plane diagram.

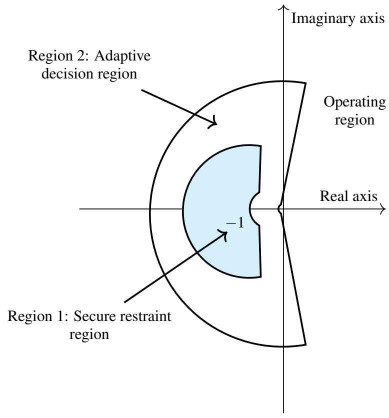

(b) Adaptive α-plane

Figure 1: α plane operating regions

2.1 Adaptive α-plane based differential protection

The adaptive α-plane method extends the conventional differential scheme mainly as its decision criterion may be compromised when the trajectory of the current ratio remains within the restraint region during a high-resistance internal fault [12]. Adaptive scheme combines the geometric information of the α-plane with complementary variables, such as the voltage–current angle and the magnitude of current variation at both terminals of the line. The α-plane is divided into three functional regions according to Fig. 1b.

Region 1 corresponds to a restraint zone intended to ensure relay blocking under normal operating conditions and during external faults. This region is defined by a restricted interval of current ratio magnitudes of $0.8 \leq |C_R| \leq 2.5$) and a wide angular margin centred around 180°, with approximate limits between 120° and 240° [12]. The design of this region ensures that, under healthy system conditions, load variations, synchronisation errors, and external faults keep the current ratio within this zone. Consequently, sustained residence of the ratio in Region 1 is unambiguously interpreted as a non-internal condition, and the relay remains blocked without the need to evaluate additional features. Region 2 surrounds the primary restraint region and represents an area of geometric overlap in the α-plane. This region extends towards higher ratio magnitudes, typically up to $|C_R| \approx 5$, while maintaining an angular margin similar to that of Region 1 [12]. Within this region, trajectories associated with high-resistance internal faults, severe external faults with CT saturation, synchronisation errors, and communication channel asymmetries may coexist. Therefore, when the current ratio falls within Region 2, the adaptive method activates additional electrical features to distinguish internal faults from external conditions. The operating region corresponds to the area of the α-plane located outside Regions 1 and 2 and represents the zone in which the relay must issue a tripping command. When the current ratio moves into this region, an unequivocal internal fault condition is identified, which may correspond to either low- or high-resistance faults, depending on the fault location and system conditions [12]. In this zone, the geometric criterion of the α-plane is sufficient for decision-making, and activation of complementary adaptive functions is not required. In this manner, the scheme ensures rapid and selective operation for the most frequent internal faults in transmission lines. To resolve the ambiguity associated with region 2, the adaptive method incorporates additional criteria to determine whether a fault or a load variation is present. These criteria consider the angle between the voltage and current and the difference between the pre-disturbance and disturbance currents, enabling reliable identification of high-resistance internal faults when the current ratio remains within this region.

2.2 Behaviour of the Adaptive Method under Fault Conditions

Under normal operating conditions and during external faults, the current ratio remains within Region 1 (secure restraint region) or Region 2 (adaptive decision region) of the α-plane. In these cases, the complementary features do not simultaneously exceed the established thresholds, and therefore the index K_1 remains zero and the relay remains blocked.

Conversely, under high-resistance internal fault conditions, although the current ratio may lie within Region 2, the combination of a large voltage–current angular deviation and a significant increase in current difference between both line terminals enables activation of the adaptive logic. In this situation, the index K_1 assumes a unit value, leading the scheme to a secure and reliable tripping decision [12].

Consequently, the adaptive α-plane method achieves a substantial improvement in differential relay sensitivity to high-resistance internal faults, without compromising robustness against external disturbances, thereby establishing itself as an advanced and effective strategy for the protection of modern transmission lines.

3. Proposed tests and result analysis

This section presents the analysis of results from the implemented α-plane-based line differential protection, evaluated across different fault scenarios. The analysis focuses on the ability to discriminate among pre-fault conditions and internal and external faults based on the behaviour of currents measured at the local and remote terminals.

Fig. 2 illustrates the test system used to obtain the results analysed in this paper. This system corresponds to a power network designed to enable comparative evaluation of line differential protection algorithms. The system includes an IBR connected at a common point of interconnection (POI), enabling operation under different supply configurations. The IBR has a rated power of 60 [MVA] at a line voltage of 66 [kV] and is interconnected through line L_1.

3.1 Testing scenarios

Testing scenarios, which include several fault types (Single-phase-to-ground, two-phase-to-ground, and three-phase-to-ground faults) at 2 s, for fault resistances of $R_f = 0\ \Omega$ and $R_f = 10\ \Omega$, and sampling frequencies of 16 and 1024 samples per cycle. In the case of two-phase-to-ground faults, for protection methods based on the α-plane and segregated phase comparison, the results obtained for faults located at the line terminals (0% and 100%) exhibited behaviour very similar to that observed when the fault was located at the midpoint of the line (50%). Similarly, in the algorithm based on the Clarke transform, fault resistances of $R_f = 5\ \Omega$ and $R_f = 10\ \Omega$ did not produce significant changes in the $\alpha\beta$ trajectory compared with the case $R_f = 0\ \Omega$. This behaviour is attributed to the fact that, in two-phase faults, the resistive component of the fault has a limited influence on the transformed differential currents, with the dynamics of phase unbalance being the dominant factor in shaping the trajectory. Owing to the similarity in the behaviour of the analysed algorithms, a criterion was adopted to simplify the presentation of results corresponding to two-phase faults. This simplification reduces redundancy without compromising the validity of the analysis. Finally, the influence of temporal resolution on the performance of the protection schemes was analysed by comparing two sampling configurations (1024 and 16 samples per cycle) and by evaluating the trade-off between the accuracy of differential quantity estimation and computational complexity. The results were analysed over the time interval from 1.6 s to 2.5 s, which covers the pre-fault and fault stages. The post-fault regime was not considered, as this thesis focuses on the performance of protection algorithms during the critical detection and decision-making stages, which are decisive for the reliable operation of line differential protection schemes.

3.2 Testing results and analysis

The most challenging fault scenarios, with respect to protection performance, are presented and analysed. Additionally, samples collected 50 ms after fault inception are analysed.

3.3 Analysis in the case of fault resistance variation

Two fault resistances of $R_f = 0\ \Omega$ and $R_f = 10\ \Omega$, for faults located at the 50% of the line L_1 at 2 s, and a sampling frequency of 1024 samples per cycle is considered for testing the conventional and the adaptive α-plane based line differential protection. The results for faults located at the

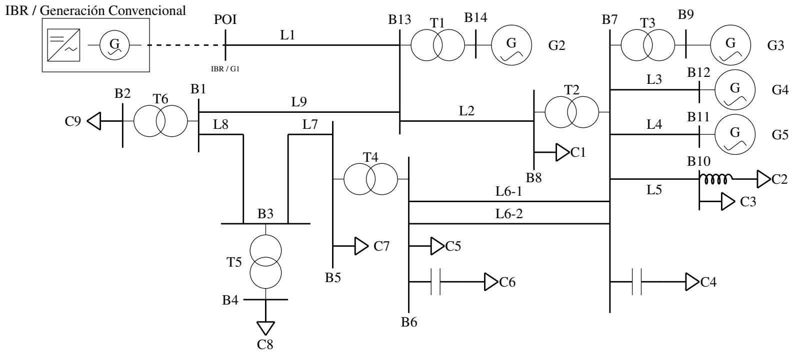

Figure 2: Single-line diagram of the test system with IBR and conventional generation.

50% of the line L_1 are depicted in figures 3 and 4, where the three upper plots correspond to the conventional and the three lower plots correspond to the adaptive α-plane based line differential protection. From the results depicted in Figure 3, the conventional and the adaptive protection approaches perform adequately. In both cases, and for a single-phase fault, the α_A value leaves the restrain region (conventional protection) and the regions 1 and 2 (adaptive protection), indicating a trip of the breaker A. The behaviour of α_B and α_C demonstrates adequate performance of the protection approach, as these variables remain within the restraint regions, avoiding false trips. In the case of three-phase faults, depicted in figure 4, the conventional and the adaptive protection approaches can experience difficulties. In both cases, the α value leaves and returns the restraint region (conventional protection) and the region 2 (adaptive protection). Additionally, in the conventional approach phase B, an undesired time delay is presented as α_B remains in the restraint region. In the same situation, the adaptive protection approach performs better as the α_B values are in the region 2, where a trip is originated as a consequence of the fault condition, avoiding undesired delays. Finally, the previous results highlight the adaptive method's greater sensitivity and faster response time.

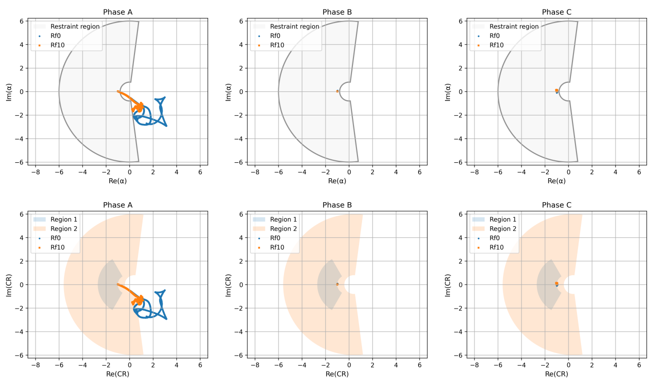

Figure 3: Protection performance in the α-plane for a single-phase-to-ground fault located at 50 % of the line L_1, considering fault resistances $R_f = 0\ \Omega$ (blue), $R_f = 10\ \Omega$ (orange), and 1024 samples per cycle.

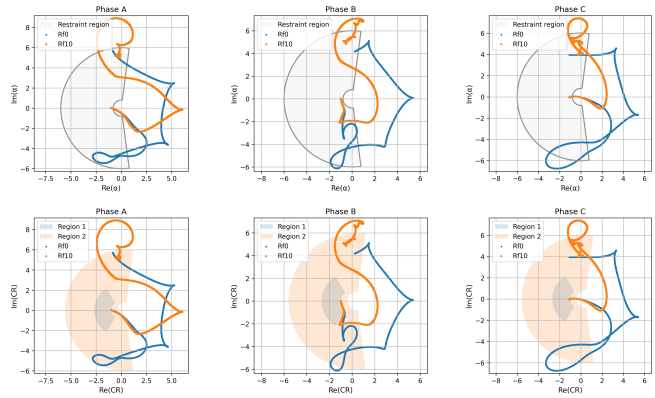

Figure 4: Protection performance in the α-plane for a three-phase-to-ground fault located at 50 % of the line L_1, considering fault resistances $R_f = 0\ \Omega$ (blue), $R_f = 10\ \Omega$ (orange), and 1024 samples per cycle.

3.3.1 Analysis in the case of fault distance variation

The results presented in figures 5 and 6 include two additional distances to those presented in section 3.3, considering faults at 0% and 100% of the L_1 length and for three-phase faults additionally. In this situation, the performance of the protection based on the behaviour of α is similar to the presented in section 3.3, figure , where protection issues are specially experienced in phase B. Similarly, the conventional α-plane based line differential protection has undesired trip delay in the case of phase B.

3.4 Analysis in the case of sampling frequency variation

This test presents α-plane based line differential protection behaviour in the case of a low sampling frequency of 16 samples per cycle. In the case of A-single-phase-to-ground fault depicted in Figure 8, the relay had an undesired delay (higher than 50 ms), reducing its performance significantly when compared to the performance in the case of higher sampling frequencies as presented in section 3.3. In the case of three-phase faults depicted in Figure 9, the protection approach also exhibits similar performance, with undesired delays that are critical for conventional α-plane-based line differential protection.

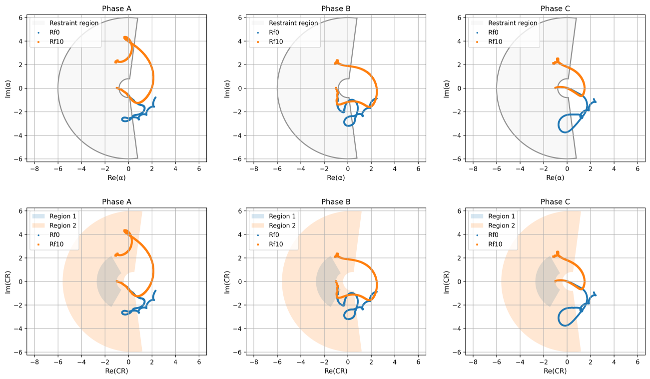

Figure 5: Protection performance in the α-plane for a three-phase-to-ground fault located at 0 % of the line, considering fault resistances $R_f = 0\ \Omega$ (blue) and $R_f = 10\ \Omega$(orange), using 1024 samples per cycle.

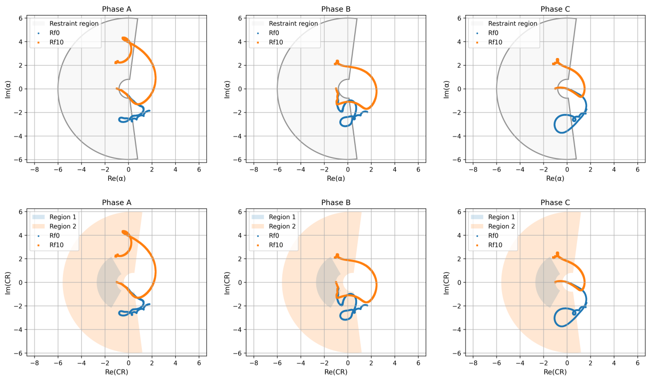

Figure 6: Protection performance in the α-plane for a three-phase-to-ground fault located at 100 % of the line L_1, considering fault resistances $R_f = 0\ \Omega$ (blue) and $R_f = 10\ \Omega$(orange), using 1024 samples per cycle.

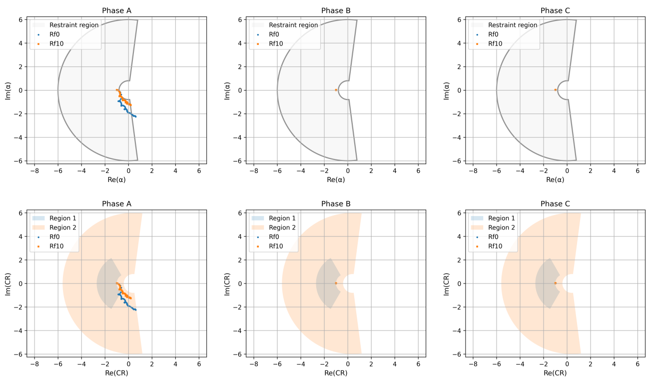

Figure 7: Protection performance in the α-plane for a single-phase-to-ground fault located at 50 % of the line, considering fault resistances $R_f = 0\ \Omega$ and $R_f = 10\ \Omega$, using 16 samples per cycle.

3.5 Analysis in the case of external faults

The performance of conventional and adaptive α-plane-based line differential protection is outstanding in the case of the external faults for all fault types, location, and fault resistances analysed. Figure 10 present the behaviour of α in the case of a two-phase-to-ground fault located at 50 % of the line L_2, considering fault resistances $R_f = 0\ \Omega$ and $R_f = 10\ \Omega$. Both the conventional and adaptive protection

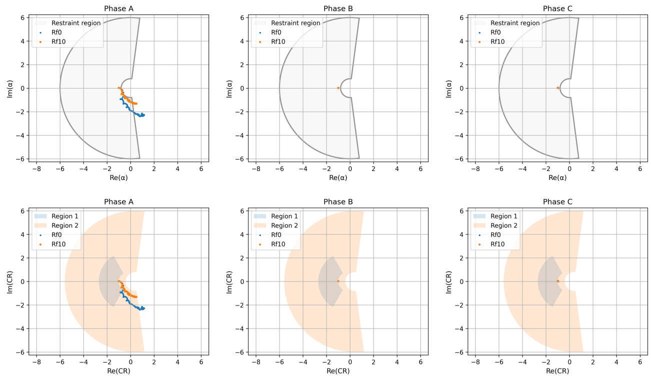

Figure 8: Protection performance in the α-plane for a single-phase-to-ground fault located at 50 % of the line, considering fault resistances $R_f = 0\ \Omega$(blue) and $R_f = 10\ \Omega$(orange), using 16 samples per cycle.

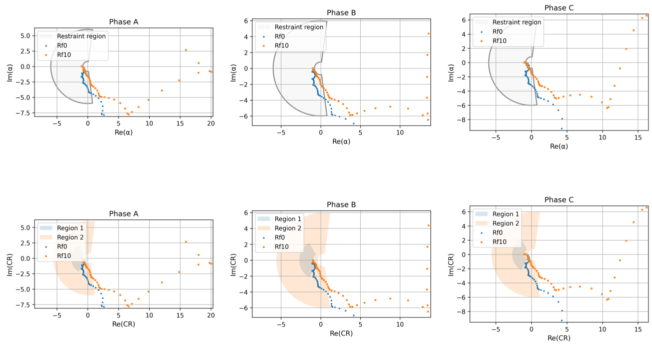

Figure 9: Protection performance in the α-plane for a three-phase-to-ground fault located at 50 % of the line, considering fault resistances $R_f = 0\ \Omega$(blue) and $R_f = 10\ \Omega$(orange), using 16 samples per cycle.

approaches perform adequately, as no trips are expected under external faults.

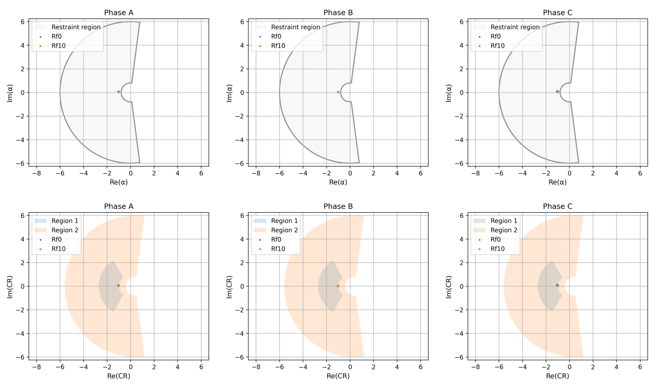

Figure 10: Protection performance for an external two-phase-to-ground fault located at 50 % of the line L_2, considering fault resistances $R_f = 0\ \Omega$ and $R_f = 10\ \Omega$, using 1024 samples per cycle.

4. Conclusion

This paper presents a comprehensive evaluation of α-plane-based line differential protection under operating conditions representative of modern power systems with high penetration of inverter-based resources (IBRs). The α-plane method was assessed through theoretical, computational, and practical analyses, which confirmed its conceptual robustness and effectiveness for fault discrimination under conventional system conditions.

The increasing integration of IBRs reveals significant limitations, particularly for the conventional α-plane-based line differential protection. These factors restrict its adaptability to highly dynamic environments characterised by power-electronic-based generation and low short-circuit capacity. In contrast, the adaptive α-plane-based line differential protection demonstrates improved performance in IBR-dominated systems by enhancing robustness. It achieves a favourable balance between sensitivity and security, ensuring reliable operation in most internal faults while maintaining selectivity under external conditions. Additionally, the analysis of different fault resistances indicates that low-fault-current conditions remain challenging for several protection techniques, emphasising the need for advanced adaptive and signal-processing strategies. Overall, while the conventional α-plane-based line differential protection remains valuable as an analytical tool, its practical applicability in modern power systems is increasingly limited. Adaptive α-plane-based line differential protection is a more suitable solution for future protection schemes in networks with high IBR penetration, and further research should focus on developing unified analytical formulations and conducting large-scale validation.

Acknowledgment

The Vicerectoría de investigación, inovación y extensión funds this research through the project *Performance evaluation of non-pilot line protection relays in power systems with converter-interfaced generation*, code 6-25-3 at the Universidad Tecnológica de Pereira. The ICE^3 research group obtained this product.

References

[1] V. A. Rosero-Morillo, F. Gonzalez-Longatt, J. M. Riquelme-Dominguez, and E. Orduña. Impact of inverter-based distributed generation integration on current seen by overcurrent relay: Cigre european mv network case. In *2023 IEEE Central America and Panama Convention (CONCAPAN XLI)*, pages 1–6, 2023.

[2] Hammad Khalid and Abdulfetah Shobole. Existing developments in adaptive smart grid protection: A review. *Electric Power Systems Research*, 191:106901, 2020.

[3] Saima Akhtar, Muhammad Adeel, Muhammad Iqbal, Abderrahmane Namoun, Ayesha Tufail, and Ki-Hyung Kim. Deep learning methods utilization in electric power systems. *Energy Reports*, 10:2138–2151, 2023.

[4] Maedeh Mahzarnia, Mohsen Parsa Moghaddam, Payam Teimourzadeh Baboli, and Pierluigi Siano. A review of the measures to enhance power systems resilience. *IEEE Systems Journal*, 14(3):4059–4070, 2020.

[5] Jie Li, Jiahui Feng, Min Huang, Shuai Liu, and Guoqing Wang. Optimal protection coordination for directional overcurrent relays in radial distribution networks with inverter-based distributed energy resources. *International Journal of Electrical Power & Energy Systems*, 167:110622, 2025.

[6] Juan Cardenas. Line protection analysis on faults in networks with high penetration of inverter-based generation. recommendations for future improvements. In *19th International Conference on Developments in Power System Protection (DPSP Europe)*, pages 1–6, 2025.

[7] Juan Cardenas. Line protection performance during faults in networks with solar pv and wind renewable energy. Technical report, Adneli Consultant, 2022.

[8] Soroush Sanati and Innocent Kamwa. A comprehensive review on differential protection schemes in ibr-dominated microgrids. *IEEE Access*, 12:170250–170271, 2024.

[9] Daniel M. Brasil, Carlos C. S. Silva, Kellen M. Silva, and Ricardo G. Bainy. On improving differential protection of lines interconnecting inverter-based resources. In *8th Workshop on Communication Networks and Power Systems (WCNPS)*, pages 1–6, 2023.

[10] Hugh Miller, John Burger, Norman Fischer, and Bogdan Kasztenny. Modern line current differential protection solutions. In *2010 IEEE Power and Energy Society General Meeting*, pages 1–9, 2010.

[11] Waldemar Rebizant, Armando Guzman, Stanley Zocholl, Zoran Djekic, and Mladen Kezunovic. Settingless protection: Feasibility study. In *19th International Conference on Developments in Power System Protection (DPSP Europe)*, pages 1–6, 2025.

[12] Saumendra Sarangi and Ashok Kumar Pradhan. Adaptive α-plane line differential protection. *IET Generation, Transmission & Distribution*, 11(10):2468–2477, 2017.

[13] Gabriel Benmouyal. The trajectories of line current differential faults in the alpha plane. Technical report, Schweitzer Engineering Laboratories, Pullman, WA, USA, 2005.

[14] Kleber M. Silva and Rodrigo G. Bainy. Generalized alpha plane for numerical differential protection applications. *IEEE Transactions on Power Delivery*, 31(6):2565–2566, 2016.